

Flow analysis of the Arctic Ocean with a complicated density field

Analyse de l'écoulement dans l'Océan Arctique en tenant compte des effets de densité

AKIRA WADA, *Nihon University, College of Industrial Technology, 1-2-1, Izumi, Narashino, Chiba, Japan*

ABSTRACT

In recent years, research has been underway to clarify the fate of radioactive wastes dumped into the Arctic Ocean (especially, the Kara Sea and the Barents Sea). These sea areas are very narrow, shallow and located close to land.

To analyze the diffusion of radionuclides and carry out exposure dose assessment by determining the circulation of seawater in these sea areas, it is necessary to identify the flow characteristics of the seas.

As the first step of research, the mechanism of flows in the Barents Sea and the Kara Sea in the Arctic Ocean was investigated. As the second step, the entire Arctic Ocean was studied.

Using the observation data (water temperature and salinity), the flow was analyzed using a hybrid box model, taking into account river flows and density structures in the seas. The results thus obtained agreed with the observed features in many aspects. Especially, stream flows in the Norwegian Sea, Barents Sea and Kara Sea showed fairly realistic features. The flow field in the surface layer in the central Arctic Ocean agreed with that in previously known data. In the intermediate and deep layers, there was a stream flow that agreed with the known cyclonic circulation. East of Greenland, a stream flow equivalent to the East Greenland Current was recognized.

RÉSUMÉ

Ces dernières années, une recherche a été entreprise pour élucider le devenir des déchets radioactifs déversés dans l'Océan Arctique (en particulier le golfe de Kara et la mer de Barentz). Ces mers sont très étroites, peu profondes, et situées à proximité des terres.

Pour analyser la diffusion des radionucléides et en déduire une estimation de la dose d'exposition liée à la circulation de l'eau de mer dans ces zones, il est nécessaire d'identifier les caractéristiques des courants marins.

Dans une première étape, on a étudié le mécanisme des écoulements dans la mer de Barentz et le golfe de Kara de l'Océan Glacial Arctique. En seconde étape, c'est tout l'Océan Arctique qui a été étudié. A partir des données observées (température de l'eau et salinité), l'écoulement a été analysé au moyen d'un modèle boîte hybride qui prenait en compte l'écoulement des rivières et les structures de densité dans les mers. Les résultats ainsi obtenus étaient en accord avec de nombreux aspects des caractéristiques observées. En particulier les courants dans la mer de Norvège, la mer de Barentz et le golfe de Kara présentaient des allures franchement réalistes. Le champ de courant de la couche de surface dans la partie centrale de l'Océan Arctique correspondait bien avec les données existantes. Dans les couches intermédiaires et profondes, le courant était en accord avec la circulation cyclonique connue. A l'Est du Groenland on a bien retrouvé un courant correspondant au East Greenland Current.

Introduction

Recently, there has been considerable interest in the dumping of radioactive wastes into the Arctic Ocean (especially, the Kara Sea and the Barents Sea) by the former Soviet Union. These seas are narrow, shallow and close to land (see Fig.1). To assess the impact of such dumping, it is necessary to establish a safety assessment method that permits the prediction of not only regional but also global-scale effects.

To analyze the diffusion of radionuclides and make an exposure dose assessment by determining the circulation of seawater in these areas, it will be necessary to identify the flow characteristics of the seas. However, little research has been conducted insofar as these sea areas are concerned. Moreover, these seas are largely ice-covered in winter, thus available winter oceanographic data are limited. In this research, the author used existing salinity and water temperature data and information such as meteorological and oceanographical data provided by IAEA.

Representatives of both IAEA and Seven Member states (Danish/Norwegian group, Japan, The Netherlands, The Russian Federation, Switzerland, United Kingdom and United States of America) were involved in the modeling, coordinated within the framework of the IAEA's International Arctic Assessment Project (IASAP). The model and assessment exercises included contribu-

tions to all the important aspects required for radiological assessment studies (Wada et al. 1997).

This paper centers on flow modeling and its analysis, which is of major significance to assessment exercises.

Using these observation data (water temperature and salinity), the water-mass characteristics of the Arctic Ocean were examined with reference to the known data, and the results thus obtained were compared with the results of flow analysis to investigate the present condition of flows in these sea areas.

Method of study

What impact will the actual dumping of radioactive waste into the Arctic Ocean have in the future? As the first step to solve this question, the author investigate the flows in the Barents Sea and the Kara Sea based on observed water temperature and salinity distributions in these seas (local scale). Based on data obtained by NOAA's observations, water temperature and salinity in the range of 64°~85° north latitude and 0°~120° east longitude were obtained and graphically represented at intervals of 0.1°C and 0.1‰ respectively, and were used to examine the oceanographical characteristics of these seas. The horizontal box size was 4°x1°, and each box was vertically divided into 6 layers (0~50m, 50~100m, 100~200m, 200~500m, 500~900m and 900~2500m). Figure 2

Revision received February 26, 2001. Open for discussion till October 31, 2002.

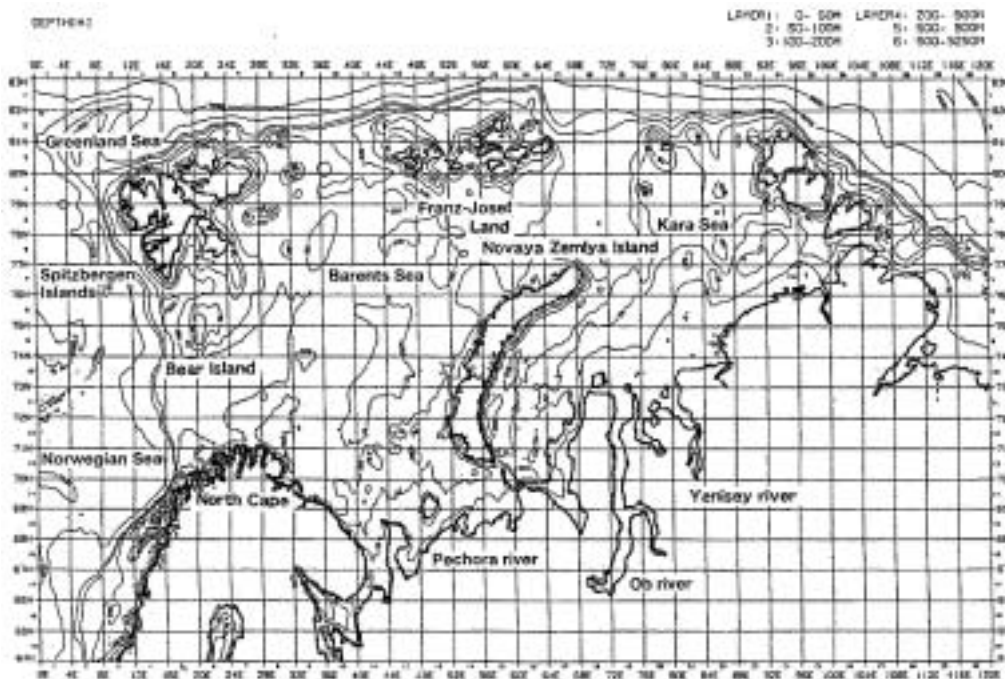


Fig. 1. The Barents Sea and the Kara Sea.

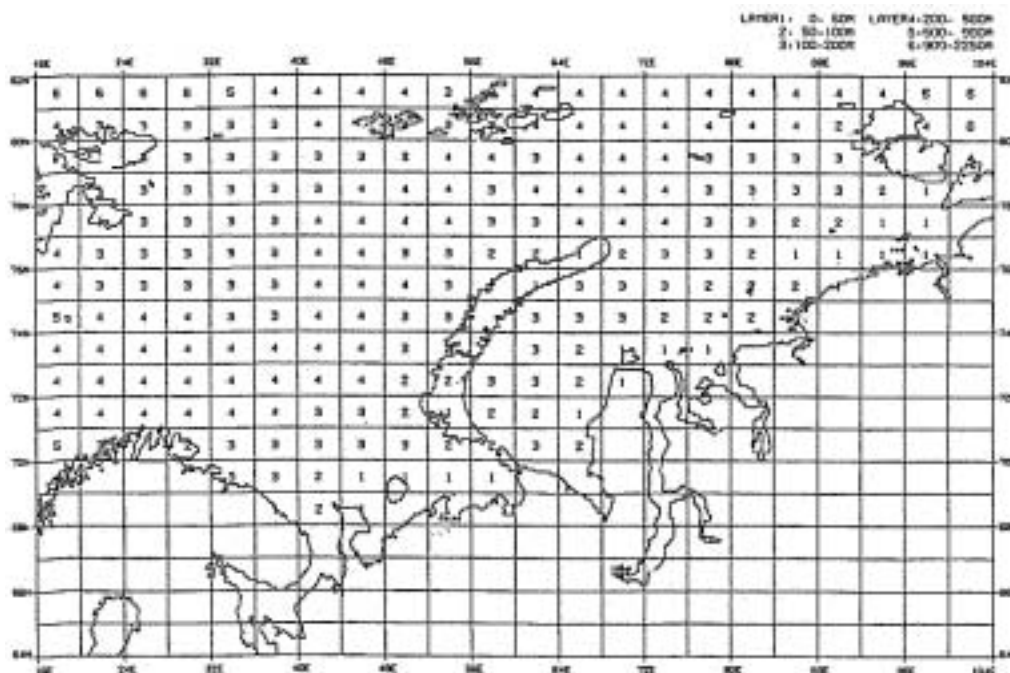


Fig. 2. Grids of the model and the number of vertical layers.

shows the grids of the model and the number of vertical layers. As the second step of research, the entire Arctic Ocean was studied, using horizontal boxes of 222 x 222km which varied with locations on the spherical coordinate system, which were divided vertically into 5 layers (0-50m, 50-100m, 100-200m, 200- 500m, and 500-4250m). (Fig. 3)

The upper 4 layers in both models have the same layer thickness. The annual mean horizontal and vertical exchange flow rates in a total of 892 compartments were calculated to examine the movement of seawater.

Density structure of Arctic seawater

Arctic Ocean (Fig. 4)

The Arctic Ocean has an area of $9.5 \times 10^6 \text{ km}^2$ with a volume of $1.7 \times 10^7 \text{ km}^3$ and it is semi-enclosed by land. Part of it is as deep as 4,000m. There are three major water masses, as described below.

- i. Arctic surface-layer water: This water mass exists up to a depth of 200m from the surface, and both temperature and salinity undergo remarkable changes depending on the ice cover.

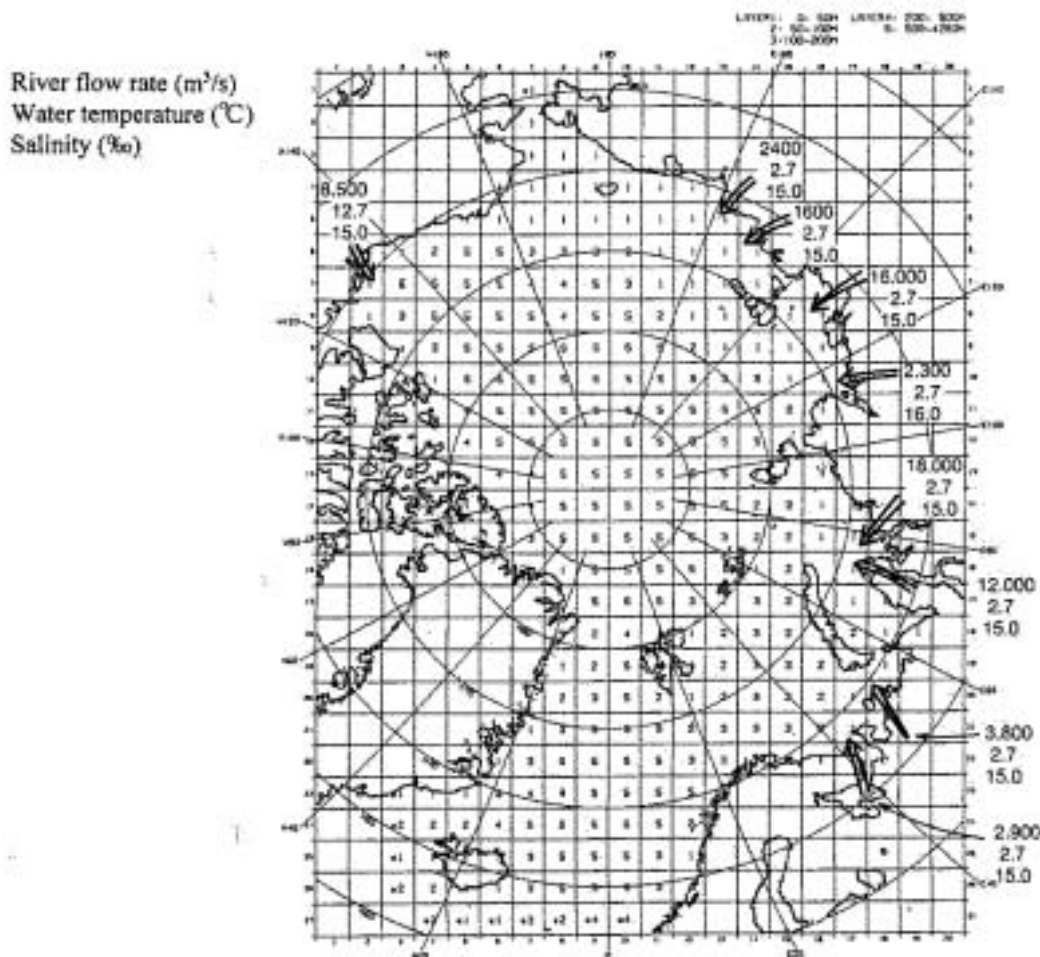


Fig. 3. Division of grid, the number of layers and river inflow positions in the Arctic Ocean.

ii. Atlantic water: This water mass exists 200~900m under the surface. Its temperature is 0°C or more, and salinity is

around 35‰.

iii Arctic deep-layer water: This water mass lies below the Atlantic water and extends down to the bottom of the ocean.

The water of the Arctic Ocean is balanced by flows which pass through the Bering Strait and the Norwegian Sea, by precipitation and river run off and by outflow to the Barents and Greenland Seas and through the Canadian Arctic archipelago.

Barents Sea

The Barents Sea has an area of $1.42 \times 10^6 \text{ km}^2$ and volume of $3 \times 10^5 \text{ km}^3$. It is largely open to the Norwegian Sea in the west and the central Arctic basin to the north. The average depth is 230m, with a maximum depth of 500m near Bear Island. The position of the Barents Sea between the Atlantic and Arctic Oceans gives it a key role to play in the transport of substances.

The Norwegian Atlantic Current which is a warm current, enters from the western side of North Cape. Then, the current is divided into two major branches. One flows eastward (coastal-current system) and the other flows into the northern central area. Cold Arctic water enters from the north between Spitsbergen and Franz-Josef Land, as well as from the north between Franz-Josef Land and Novaya Zemlya (see Figs.1 and 5). The water circulation in the Barents Sea is generally counter-clockwise (Harms



Fig. 4. Basins of the Arctic Ocean (Walker O.Smith, Jr, 1990).

1992, Pavlov et al. 1995).

The Barents Sea undergoes stratification in spring and mixing in winter. This sea area is high in biological production. Salinity is 32~35‰.

The Barents Sea has four major water masses as shown in Figure 5(1), identified by numbers in circles.

- ① The Atlantic water mass entering from the west as a surface-layer current,
- ② The Arctic water mass which enters as a surface-layer current from the north,
- ③ The Coastal water mass entering from the continent,
- ④ The Barents Sea water mass which stays there after mixing.

Judging from the shape of isopycnic lines, the density field is more strongly affected by the salinity field than by the water temperature field, though in the Barents Sea a sharp temperature gradient has a significant effect. The basic structure of the density distribution remains unchanged year-round.

The density of seawater is highest in the central part of the Barents Sea and in the sea area where the Atlantic water, southwest of Spitsbergen flows north along the continental shelf, showing $\sigma(s, t, p_{25})$ value of about 28. In the northernmost and southernmost parts of the Barents Sea, the density of seawater is about 0.5 lower in $\sigma(s, t, p_{25})$ due to the effects of relatively light Arctic surface-layer water and coastal water, respectively. (For $\sigma(s, t, p_{25})$, refer to the footnote.)

Kara Sea

The Kara Sea is $8.8 \times 10^5 \text{ km}^2$ in area and $9.8 \times 10^4 \text{ km}^3$ in volume. It is rather shallow; its mean water depth is 120m. However, deep valleys exist, namely, the Novaya Zemlya Trough (300~400m) east of Novaya Zemlya, and a trough (600m) north of Novaya Zemlya. In this sea area, there are inflows of river water amounting to $1,500 \text{ km}^3$ annually, mainly from the Ob and Yenisey. These fresh water inflows cause a northward flow, forming eddies which are then branched into a northeastward-flowing current along the continent and a southwestward-flowing current along the coast of Novaya Zemlya.

River water inflows are conspicuous in summer, and decrease remarkably in winter. Figure 6 shows monthly changes in major river water runoffs. The structure of water masses in the Kara Sea is dominated by water inflows from the Arctic Ocean and the Barents Sea as well as by river water inflows. Five major water masses exist in this sea. (See Figure 5(1); these water masses correspond to the numbers in triangles).

- △1 Barents Sea water originating from Atlantic water which has much higher water temperature and salinity is supplied from the north, northwest between Franz-Josef Land and Novaya Zemlya; and from the southwest through the strait south of Novaya Zemlya,
- △2 Surface-layer water in the Arctic Ocean,
- △3 The surface water of the Kara Sea,
- △4 Inflow of low-salinity water from the Ob and Yenisey rivers and relatively high-temperature ($7 \sim 10^\circ\text{C}$) water in summer.

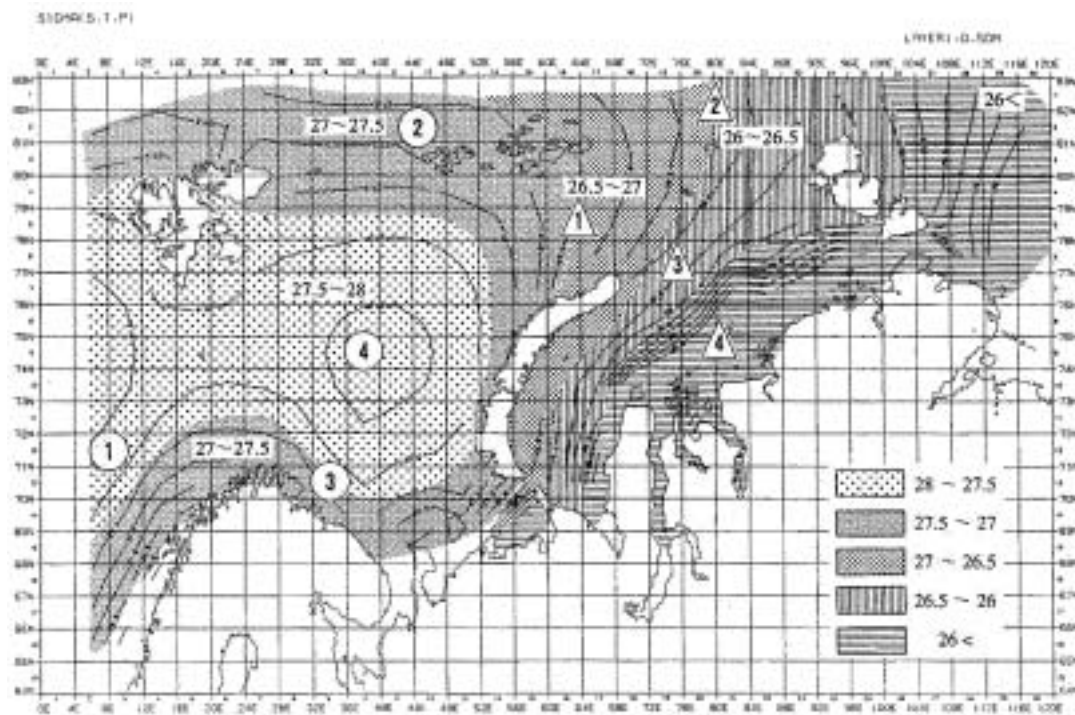


Fig. 5(1). Density distribution (0-50m layer, warm weather season).

The density of seawater $\rho(s, t, p)$ is a function of salinity s , temperature t and pressure p . In actual computation, field density $\sigma(s, t, p) = \sigma(s, t, p_{25})$ is used. $\sigma(s, t, p_{25})$ means field density at a pressure of 25db.

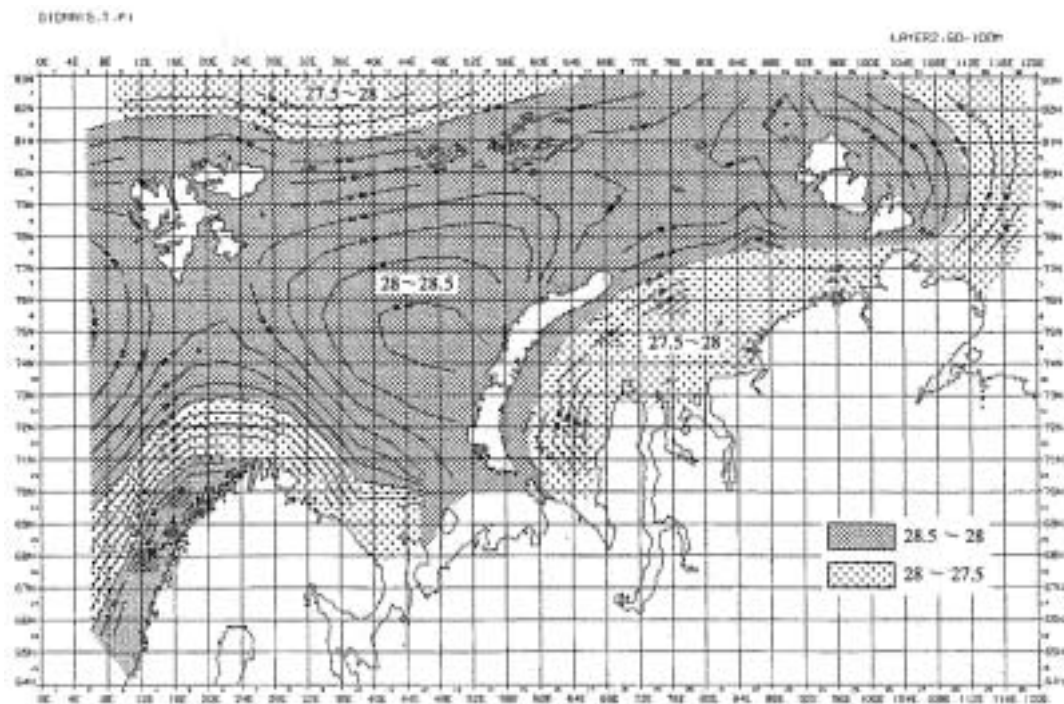


Fig. 5(2). Density distribution (50-100m layer, warm weather seas).

Salinity is 32‰ offshore and 10‰ near the mouths of the Ob and Yenisey rivers.

The Barents seawater, having high density, reaches the Kara Sea with its density reduced as it advances eastward. The density of seawater in the central part of the Kara Sea becomes about 1~1.5 lower in σ (s,t,p₂₅) in comparison with the Barents Sea.

The low-density water in the Kara Sea is formed by Arctic surface water entering from the north and a vast amount of fresh water entering from both the Ob river and the Yenisey river. Over the continental coast of the Kara Sea, a front is formed with density σ (s,t,p₂₅) falling below 26.

H. Loeng et al. (1991) point out that the three major water masses, namely, coastal water, Atlantic water and Arctic water, are related to ocean current systems. According to Fig. 7 (Loeng et al. 1991), which shows the distribution of water masses in the Barents Sea, correspondence to the density distribution shown in Fig. 5 is good.

Freezing continues for more than half of the year in this regions. The effect of wind on the flow has never been calculated.

B. Gjevik and T. Straume (1989) numerically calculated the tides in the North Sea, the Norwegian, Greenland and Barents Seas, and the Arctic Ocean. They concluded that in these sea areas the effect of tides is small, with the exception of coastal areas.

Method of flow analysis

A careful consideration must be used in the selection of an appropriate flow analysis technique for the regions having a large inflow of river water from the inland part, high- temperature and high-salinity Atlantic water masses from the western sea areas, low-temperature and high-salinity Arctic seawater from the north, large water depths and complicated topography, as seen in the Arctic Ocean.

To analyze the concentration of radionuclides extending as long as several hundred years following the flow analysis, the conservation of mass not only in each calculation box but also as a whole system must hold. That is to say, it is necessary for the following equation to hold;

$$\sum_{iB,iC} (W_{iB,iC}\rho_{iB} - W_{iC,iB}\rho_{iC}) + (\text{river inflow}) + (\text{precipitation}) - (\text{evaporation}) = 0$$

Where, iB: box number in ocean boundary, iC: box number in calculation box, $W_{iB,iC}$: exchange flow rate which enters from box iB to box iC, $W_{iC,iB}$: exchange flow rate which enters from box iC to box iB, ρ_{iC} : density of seawater in calculation box iC, ρ_{iB} : density of seawater in box iB,

$\sum_{iB,iC}$: sum for all groups (iB, iC) of boundary box and calculation box.

There are two kinds of models to cope with the flow and the dispersion of radionuclides by advection and diffusion, namely compartment or box models and hydrodynamic circulation model. Compartment or box models provide long time, spatially averaged capabilities, and some uncertainties remain in some key parameters. Hydrodynamic models provide locally resolved, short time-scale results and can only be run for limited time-scales of the order of tens of years.

In the hydrodynamic models, the circulation pattern and eddy diffusivities in the model, by trial and error, are adjusted until the observed temperature and salinity distributions can be generated by the model.

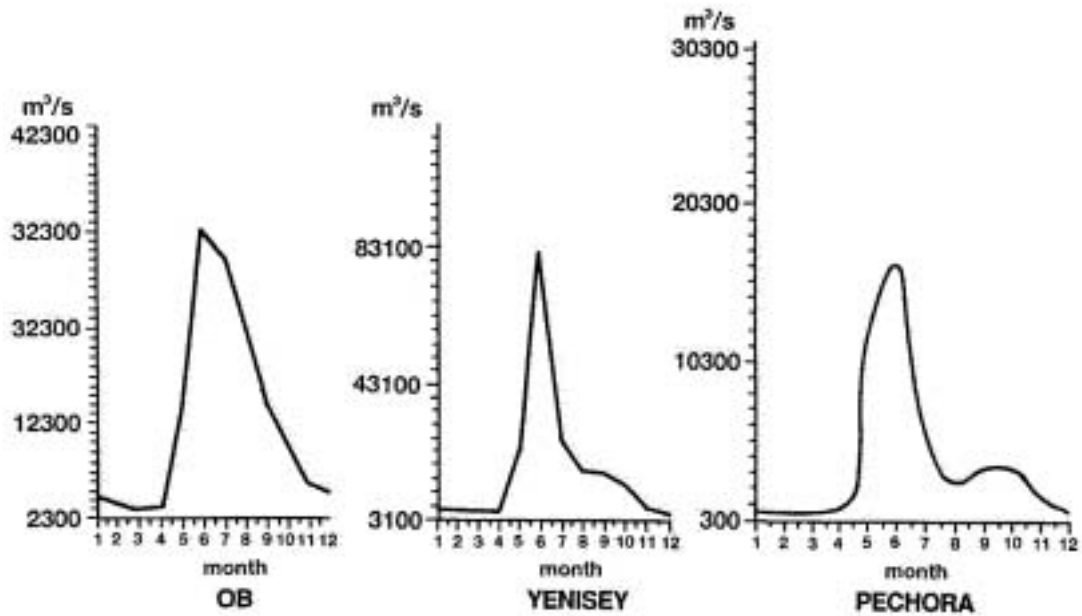


Fig. 6. Average annual cycle of river discharge to the Kara Sea and the Barents Sea.

Moreover, there is a major shortage of quality forcing data for hydrodynamic models applied to the Arctic Ocean.

Temperature and salinity are tracers ; they are the easiest of all to measure; we have much better coverage of the ocean for them than anything else; and their immediate relation to the density field means that they must be the central focus of any effort to understand the flow circulation.

The development of compartment or box models using inverse and related methods is an attempt to shift the emphasis from the scenario-based methodology to one whose emphasis is more upon

the numerical quantitative testing of data against the known equations of fluid dynamics.

In oceanography, inverse method were used for a variety of applications, including the inference of ocean current using known tracer distributions (C. Wunsch(1996), W. J. Emery and R. E. Thomson(1998)).

In this research, the method of analysis based on the box (compartment) model was selected because the depth of water in the boundary section of computations is large and it is easy to establish boundary conditions for pressure. Another reason was that it

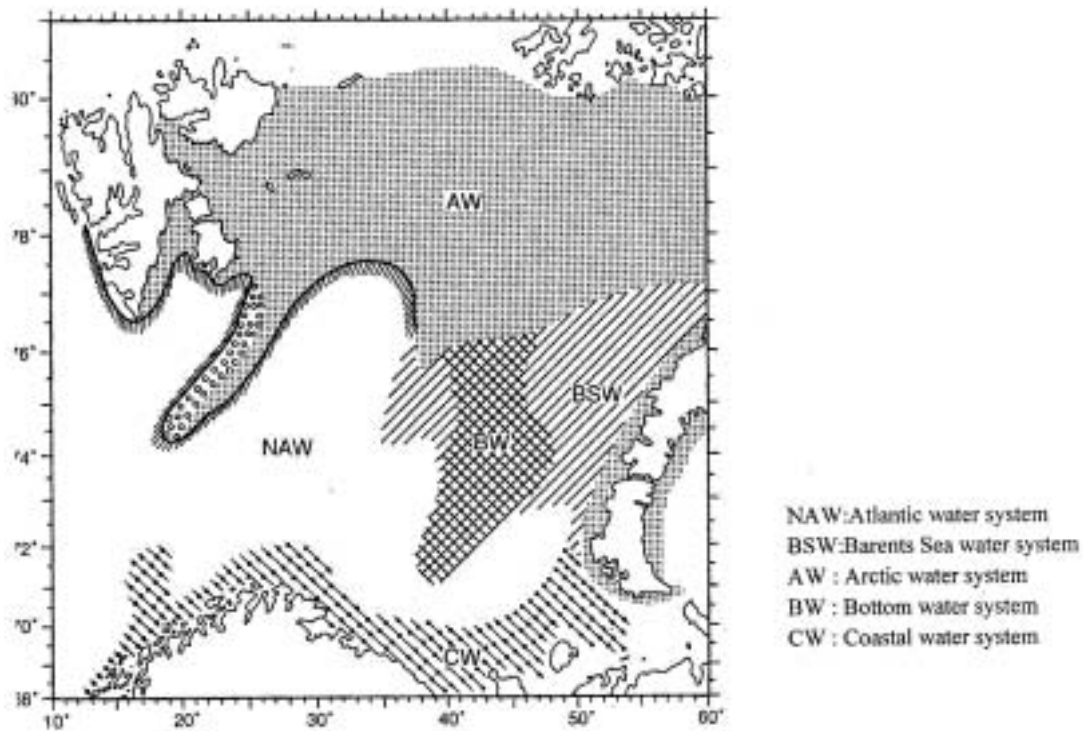


Fig. 7. Distribution of water masses in the Barents Sea (Loeng et al. 1991).

was impossible to clearly determine the flow driving forcing in the sea areas concerned for the hydrodynamic circulation model. In contrast to previous models of this type the model used in this paper is an approach for applying conservation of mass with high accuracy not only in each calculation box but also over the whole system. This model is named a hybrid box model (IAEA Report 1998), intermediate between the box model and the hydrodynamic model developed by the OECD/NEA and IAEA (IASAP) modeling groups.

The method developed in this report has been developed to cover the local (Kara and Barents Seas) and regional fields (Arctic Ocean).

Flow analysis by a hybrid box model

In this analysis, the flow which permits reproduction of the observed distributions of water temperature and salinity is mathematically calculated, to subsequently deal with the diffusion of nuclides.

The balance equations of seawater, salinity and heat volumes in each box are used to determine the exchange flow rate between boxes (Fig.8). As the number of unknown quantities becomes larger than the number of equations, however, mathematical methods such as non-linear programming are used.

For box i , the following are the conservation equations:

(1) Equation of conservation of seawater mass

$$\sum_{j \neq i} W_{ij} \rho_j - \sum_{j \neq i} W_{ji} \rho_i + \sum_r R_{ri} \rho_r + P_i - E_i = 0 \quad [\text{tons/s}] \quad (1)$$

Where $W_{ij} \geq 0$: exchange flow rate from box i to box j [m^3/s], ρ_i : density of seawater in box i [ton/m^3], obtained by Knudsen's formula from water temperature and salinity, ρ_r : density of river water in river r [ton/m^3], R_{ri} : inflow of river water from river r to box i [m^3/s], P_i : precipitation into box i [ton/s], E_i : evaporation from box i to the atmosphere [ton/s].

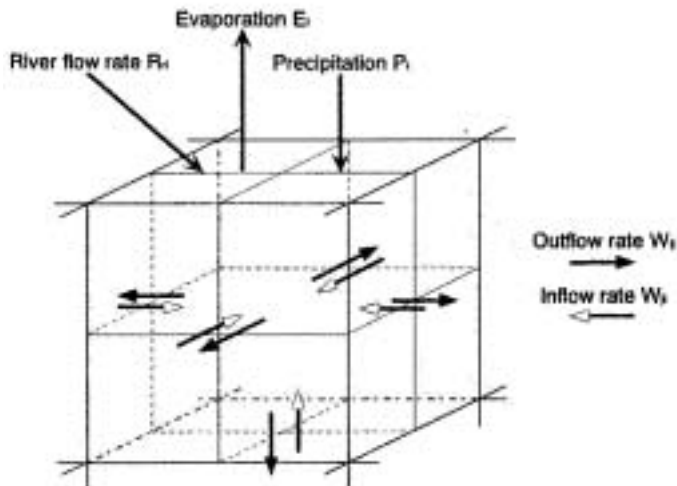


Fig. 8. Outline of the hybrid box model.

(2) Equation of conservation of salt

$$\sum_{j \neq i} W_{ij} \rho_j S_j - \sum_{j \neq i} W_{ji} \rho_i S_i + \sum_r R_{ri} \rho_r (S_r - S_i) = 0 \quad [\text{ton/s}] \quad (2)$$

S_i : salinity in box i [‰], S_r : salt in river r [‰]

(3) Equation of conservation of heat

$$\sum_{j \neq i} W_{ij} \rho_j T_j C - \sum_{j \neq i} W_{ji} \rho_i T_i C + H_i = 0 \quad [\text{M cal/s}] \quad (3)$$

T_i : water temperature in box i [$^{\circ}\text{C}$], H_i : heat entering from the atmosphere into box i [Mcal/s], C : specific heat of seawater [$\text{cal}/\text{g}\cdot^{\circ}\text{C}$], which is presently set at 1.0.

Three equations are written in matrix form as;

$$A \underline{W} = \underline{b}$$

Where A is the property matrix containing ρ , ρS and CT , \underline{W} is the vector of exchange flow rates and \underline{b} is the vector of sources and sinks.

These solutions can be expressed as the sum of a particular solution such as the least squares solution which is determined by the sources and sinks, and a series of null space solutions which are independent of the sources and sinks.

So far, the least squares solution was considered to be the most useful point since it represents the flow pattern corresponding to the minimum energy in the ocean.

Attempts in using a box model have been made to use the observed temperature and salinity distributions in the Atlantic Ocean to derive a flow pattern. In conclusion, this experience with inverse techniques on the large systems such as this research showed that this has been done with the solution containing both negative and positive exchange flow rates. The difficulty in obtaining a positive solution by requiring an exact fit to the observed data is probably due to the existence of temperature and salinity gradients within the model that can only be sustained by a negative exchange flow rate.

The difficulty in finding a solution was that the exchange flow rate must be non-negative (positive or 0) owing to the nature of the model. Therefore, one cannot use a simple linear equation or general inverse matrix representation and has to rely on a non-linear programming method with constraint (non-negative condition). That is to say, one does not require equations (1) to (3) to hold strictly and permits some minimizing errors.

In order to overcome this difficulty, non-negativity constraint was set for the exchange flow rate, $\underline{W} (\underline{W} \geq 0)$, and an efficient program was developed based on solution algorithm by mathematical formulation using a non-linear programming. This method is identical with solving a quadratic programming problem so as to minimize the objective function under the condition of non-negative exchange flow rate. That is,

Objective function (square of residual norm):

$$\|AW - \underline{b}\|^2 \rightarrow \min.,$$

and Constraint: $\underline{W} \geq 0.$

Where

- A : m×n matrix of coefficients, determined by observation data,
- \underline{b} : m – dimension constant vector determined by boundary conditions,
- \underline{W} : n – dimensional vector of exchange flow rates,
- $\| \cdot \|$: Euclidean norm,
- m : number of conservation equations, and
- n : number of exchange flow rates.

If the non-linear programming method with constraint is used, a solution can be obtained and the exchange flow rate thus obtained is non-negative, and errors in equations (1) to (3) are minimum.

$$e = \sum_i \{ \alpha_1 (\text{the left side of the equation of conservation of mass (1) in box } i)^2 + \beta_1 (\text{the left side of the equation of conservation of salt (2) in box } i)^2 + \gamma_1 (\text{the left side of the equation of conservation of heat (3) in box } i)^2 \}$$

Then, e is a function of the exchange flow rates W_{12}, W_{13}, \dots and is the sum of squares of error in the conservation equations. Exchange flow rates W_{12}, W_{13}, \dots may be obtained under the non-negative condition $W_{12}, W_{13}, \dots > 0$ to minimize the error function $e = e(W_{12}, W_{13}, \dots)$. This problem is usually called NNLS (Non-Negative Least Squares). Of the three equations of conservation, the unit of the first two

equations is [tons/s], and that of the last equation is [Mcal/s]. Adjustment is, therefore, necessary when considering the weight of the three equations. For this adjustment, α_1, β_1 and γ_1 are set as weight constants ($\alpha_1 = 10^9, \beta_1 = 10^4, \gamma_1 = 1.0$). The values of $\alpha_1, \beta_1, \gamma_1$ above were decided by taking into consideration the agreement between results of current analysis and observation data of the Pacific ocean and Tokyo Bay. For solution procedures to obtain the exchange flow rate, W, see Appendix. Refer to C. L. Lawson and R. J. Hanson(1995) for more details.

Model validation is important. A comparison was made between literature values of water fluxes in the Arctic Ocean and values obtained from the hybrid box models.

The validation process for the hybrid model has been severely restricted by the lack of appropriate flow data particularly within the Arctic area.

In the past, flow analyses were conducted in Tokyo Bay under the same input condition such as heat budget process, inflow rate of river waters, temperature and salinity distributions, using both the hybrid box model and 3D hydrodynamic model, thus confirming that there is no major difference in the results of flow circulation pattern obtained by both models (Wada, A. et al. (1996)).

On the other hand, the study was conducted focusing on the Sea of Japan using the hybrid box model to elucidate the seasonal flow characteristics under the input conditions like inflow of Tsushima Warm Current, temperature and salinity data, heat budget process and inflow of river water from the inland area (Takahashi, Y. and A. Wada (1999)).

The seasonal strengths of the Nearshore Branch of the Tsushima Warm Current, the East Korean Warm Current and the Liman Current were reproduced in the model.

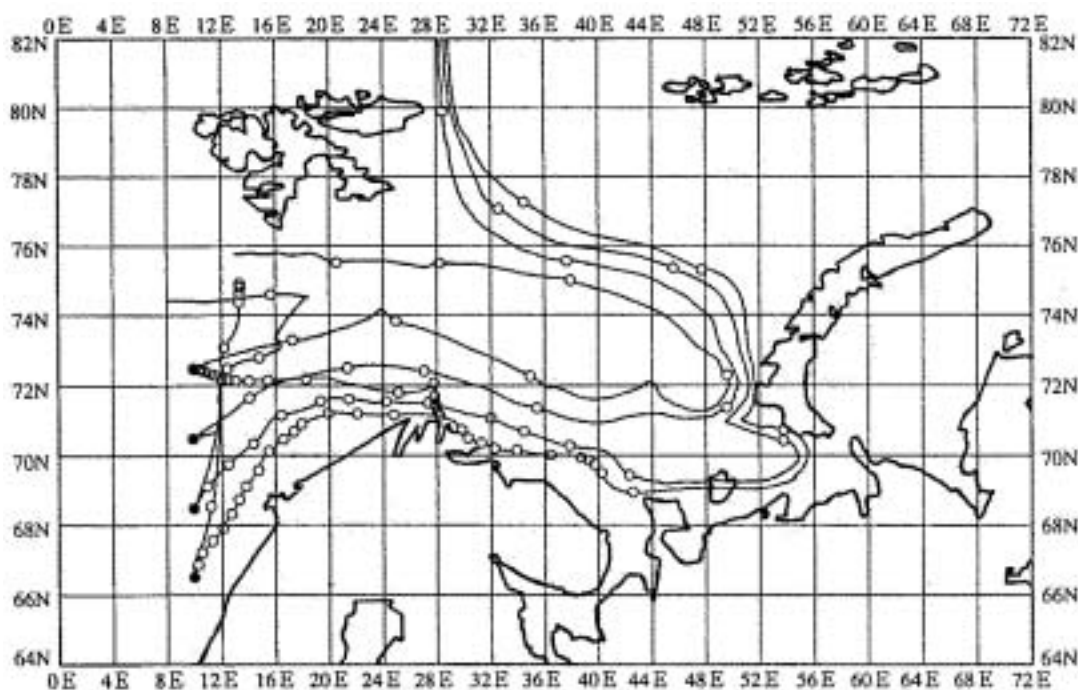


Fig. 9(1). Results of tracking (surface layer) (• : Particle injection point, o : Position of particles injected every 50 days)

The hybrid box model was applied to the safety evaluation in a hypothetical submergence accident onto the seabed in the Pacific Ocean. Agreement was found to be good by comparison of the results of current analysis and the existing knowledge on the ocean currents (Watabe, N. et al. (1996)).

Results of flow analysis in the local field

Based on the flow velocities obtained from exchange flows in the hybrid box model, particles from each box and river mouth in the Arctic Ocean were tracked and the movement of seawater particles was studied.

Barents Sea (Fig. 9(1))

The current directions shown in Fig.10 are valid for whole water column in most of the Barents Sea. Current measurements show only small changes in current direction with depth (Johansen et al. (1988); Loeng (1996)).

According to the results of tracking (Fig. 9(1)), the Atlantic water which enters the Barents Sea along the Norwegian Peninsula circulates counterclockwise in the Barents Sea and then flows through the central Arctic Ocean. This flow is in agreement with previously known data (see Fig. 10).

Generally-known flows include the current which flows from east to west between Franz-Josef Land and Novaya Zemlya, and the current which enters from the deep central Arctic Ocean known as the East Spitsbergen Current. The results obtained by tracking these flows are shown in Figure 9(2).

In the 50-100m layer in spring and summer, the current which enters the Barents Sea from the Arctic Ocean turns clockwise in the central Barents Sea and reaches the Norwegian Sea through the northern part of Bear Island, and the current which enters

from the Norwegian Sea, turns counterclockwise in the neighborhood of Bear Island and reaches the Norwegian Sea, can be observed conspicuously.

Kara Sea (Fig. 9(2))

Fig. 11 shows schematic flow pattern in the Kara Sea (Pavlov, V. K. et al. (1995)).

The northern sea area has a current which enters from the central Arctic Ocean along trenches of 80 to 125m deep and current which flows into the Barents Sea between Franz-Josef Land and Novaya Zemlya. The inflow from the central Arctic Sea to the Kara Sea in the second layer (50~100m) and third layer (100~200m) were reproduced successfully by tracking.

The western Kara Sea has the Novozemel'skaya Current which flows from northeast to southwest along the east coast of Novaya Zemlya. The results of tracking are shown in Fig. 9(2). This figure clearly shows that particles advance southward along the east coast of Novaya Zemlya.

The currents flowing north from the river mouths can be observed clearly.

Results and discussion

Seawater particles move predominantly in horizontal directions while their vertical movement is small.

The results of flow analysis were compared with the migration routes of cod (Haddock and Barents Sea cod) to examine the reproducibility of the results. It is generally considered that Haddock cods live in 4 to 10°C water.

The sea areas which meet these conditions in the Barents Sea are the coastal area and the Atlantic water mass, with high water temperatures. The migration routes observed are shown in Fig. 12.

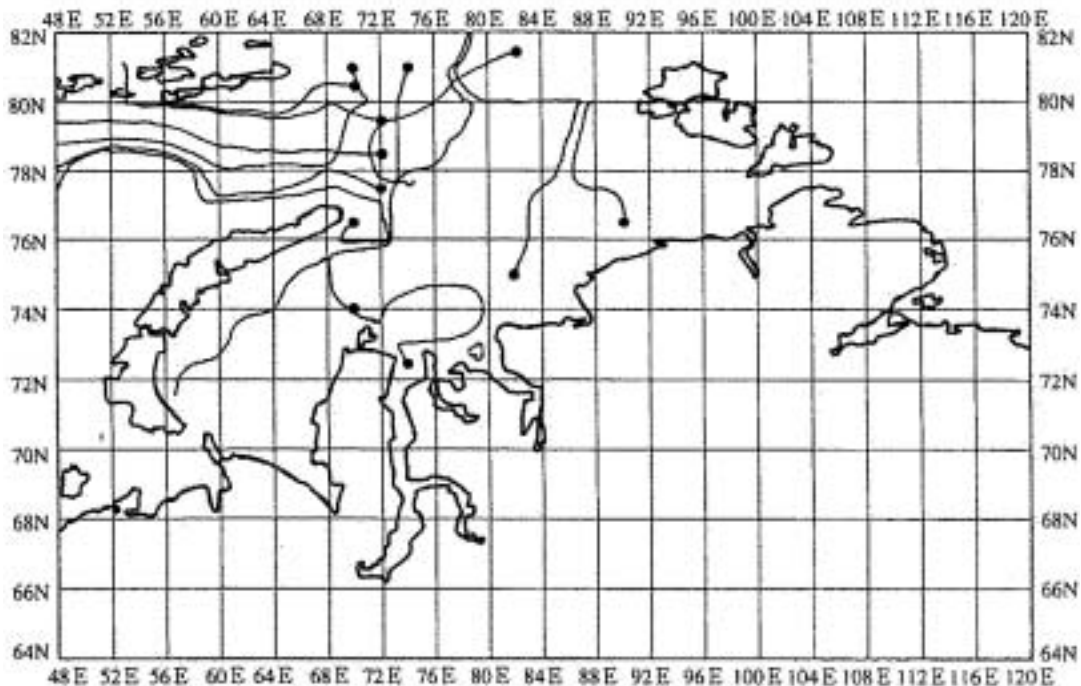


Fig. 9(2). Results of tracking (surface layer) (• : Particle injection point).

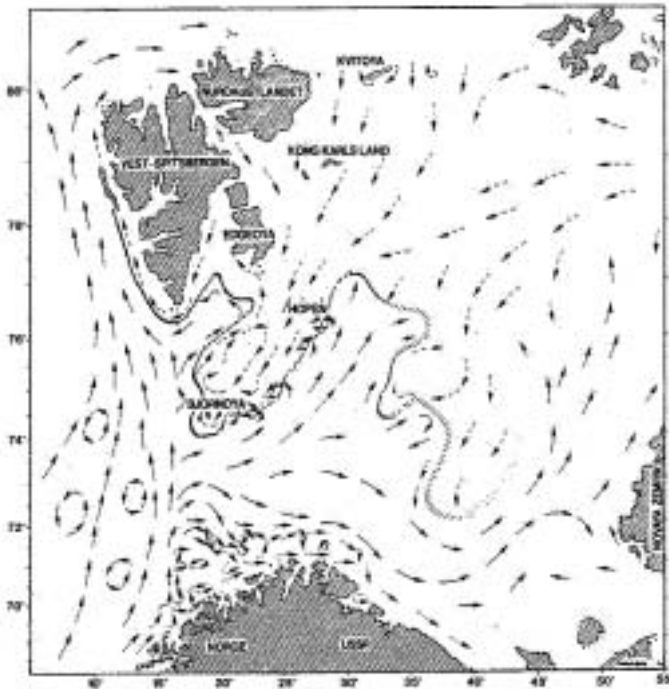


Fig. 10. Surface-layer flow patterns in the Barents Sea (H.Loeng et al. 1991)

- ▶ Atlantic ocean current system
-▶ Coastal current system
- - - - -▶ Arctic current system

The migration routes of Haddock and Barents Sea cod were compared with the results of flow analysis by the hybrid box model (Fig. 9(1)). High similarity is recognized. In particular, the route of cods entering the Barents Sea from along the coast of Norway and migrating along the continent agrees with the tracking result. Possibly, Haddock and Barents Sea cod migrate along the Norcup Ocean Current, the Mullman Coastal Current, or the Mullman



Fig. 12. Routes of eastward migration of cod in the Barents Sea (Maslov, 1944)

- ▶ Migration of mature cod
-▶ Migration of immature cod

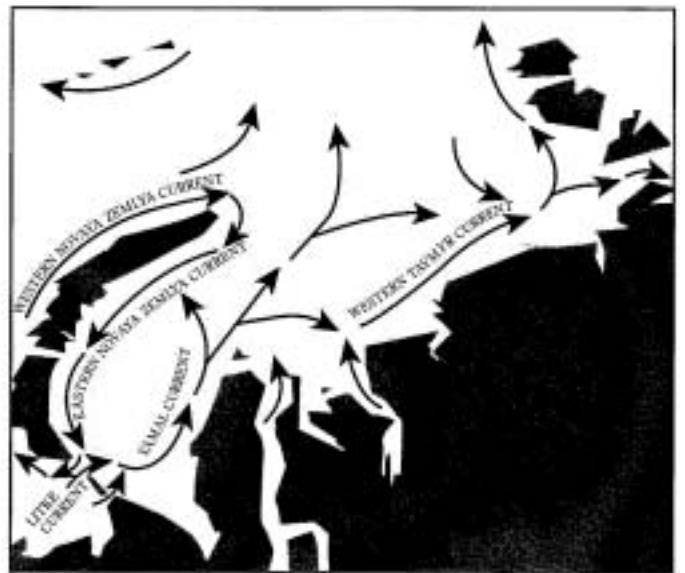


Fig. 11. General circulation in the Kara Sea (Pavlov, V.K. & S.L. Ptirman 1995).

ocean current.

Comparison of the model's current field with the observed surface velocity map indicate that the basic circulation pattern in the Barents Sea and the Kara Sea is captured by the model.

Results of flow analysis in the regional field (the whole Arctic Ocean)

Let us now compare the results of flow analyses in the Arctic Ocean with available data (mainly surface flows). Here, the author examine the velocity field at three different depths in the model.

The circulation of the surface waters of the Arctic Ocean is increasingly well understood based on studies of sea-ice drift. The prominent long-term features of the Arctic ice drift are the anticyclonic Beaufort Gyre occupying most of the Canadian Basin and the Transpolar Drift Stream flowing from the pole toward Fram Strait (Figs. 4 and 13).

The surface circulation in the model is shown in Fig. 14 (1). The deeper parts of the Arctic Ocean as depicted in Fig. 14 (2) and 14 (3) behave differently from the surface current. The anticyclonic Beaufort Gyre of the upper layer is no longer present at these depths.

In Fig. 16, the behavior of seawater particles in the vertical direction along five measuring lines in the Arctic Ocean shown in Fig. 15 is illustrated.

Fig. 17 and 18 show the track of seawater particles, based on the results of current analysis applied to these sea areas.

In Fig. 17, it is illustrated that a seawater particle in the Norwegian Sea (in the first layer) enters the Barents Sea, where it circulates anticlockwise, and that it submerges to the second layer in the south of Spitsbergen.

Then the particle goes northward in the West Spitsbergen Current, and turns to the south by the East Greenland Current (EGC) flowing southward. The particle flows further toward the North



Fig. 13. Observed flow patterns in the Arctic Ocean (Pickard, G.L. and W.J. Emery (1990)).

Atlantic Ocean, moving to the third layer.

In Fig. 18, a seawater particle deposited at the surface near the North Pole moves to the second layer as it passes between Franz-Josef Land and Novaya Zemlya Island, and abruptly turns toward the west. As in the case of Fig. 17, it then moves to the third layer and flows southward.

Vertical movements of water particles occur mainly between the first and third layers. Line(1-1') in Fig.16 clarifies the behavior of seawater particles in the vertical direction.

(1) Norwegian Sea and Greenland Sea (Figs. 14, 16, 17 and 18)
The Atlantic water inflow splits into two branches south of Spits-

bergen.

– In the Norwegian Sea, there is a northward current corresponding to the Norwegian Current (North Atlantic Ocean flow in a broad sense). One branch of this current flows north along the northern coast of Scandinavia and enters the Barents Sea, thus agreeing with the observed features (Hunkins 1990).

The other branch of the Atlantic water enters the Arctic Ocean through the Fram Strait in the West Spitsbergen Current (WSC), on the east side of the Greenland-Spitsbergen gap. Upon entering the Arctic basin, WSC encounters the southward flow. Hence, sensible heat carried by the WSC is used to melt ice, resulting in a cooled freshened water. Much of the Atlantic

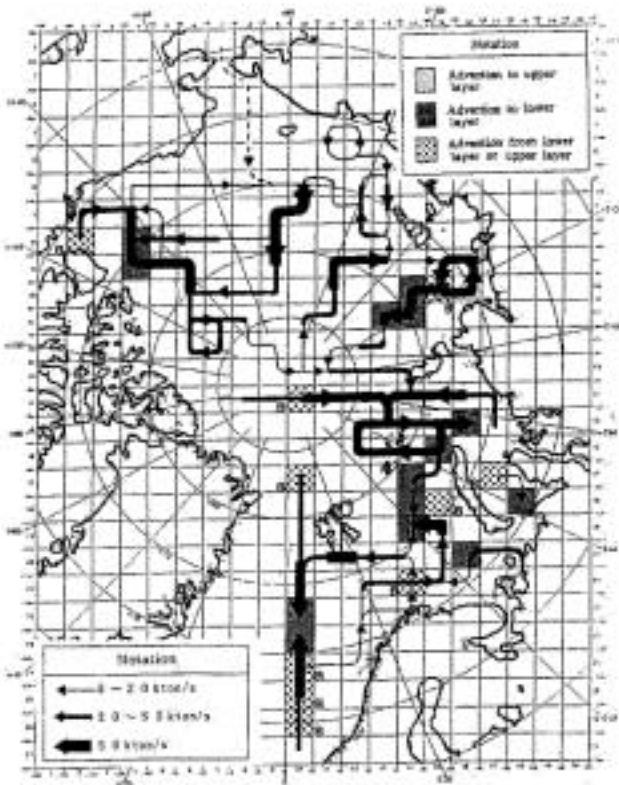


Fig. 14(1). Flow patterns in the surface layer. (0-50m)

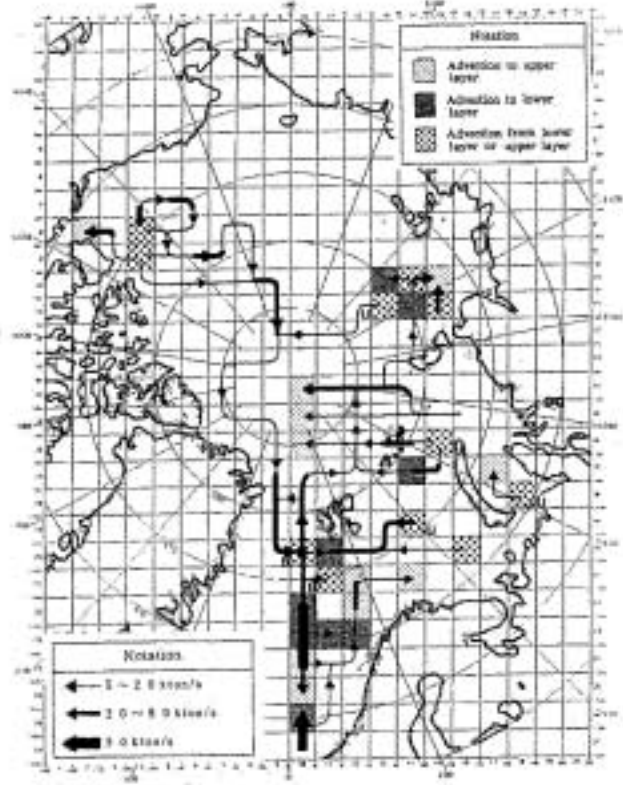


Fig. 14(2). Flow patterns in the second layer (50-100m).

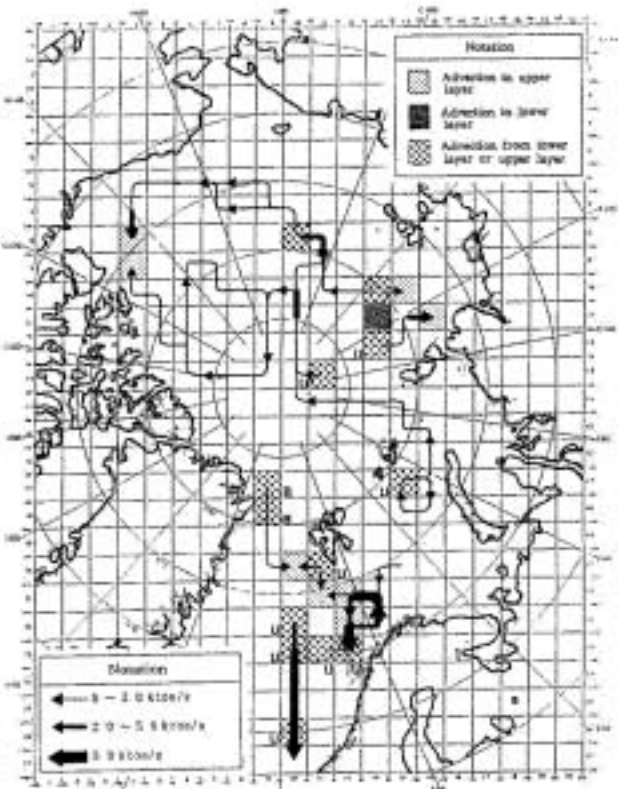


Fig. 14(3). Flow patterns in the third layer. (100-200m)

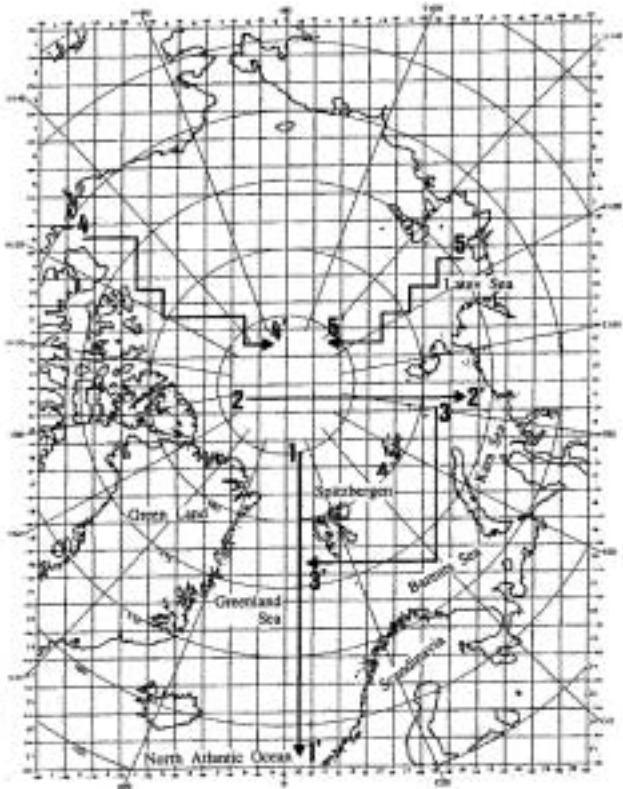


Fig. 15. Five measuring lines for studying the flow patterns

water joins the southward flowing East Greenland Current (EGC) to flow back.

- In the second and third layers (50-200m deep), the water mass

which has come up north from the southern Norwegian Sea and part of the water mass which has come out of the Barents Sea pass through the circulating current zone and enter the

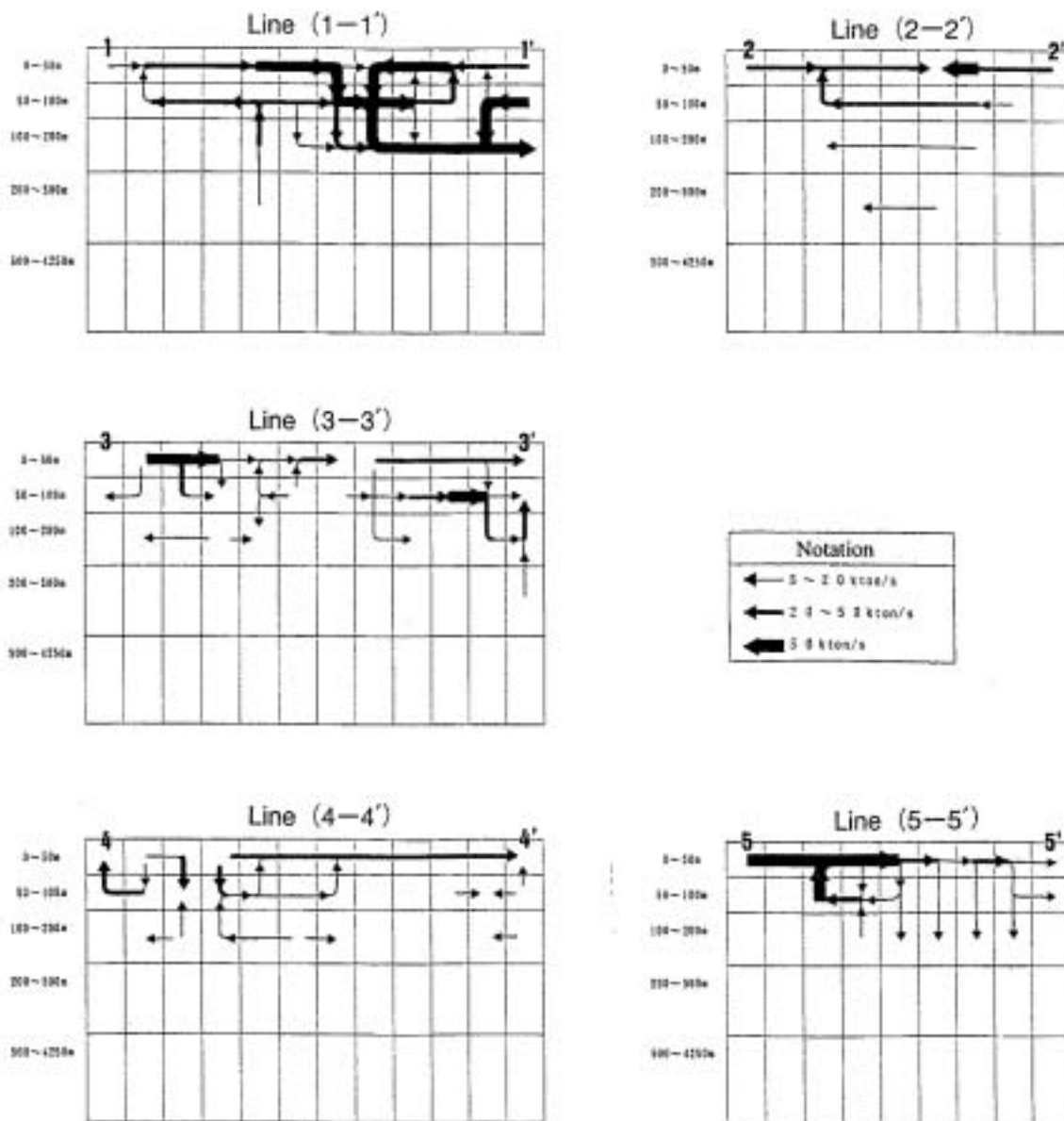


Fig. 16. Schematic diagram of flows in the vertical direction.

Arctic Ocean from west of Spitsbergen.

- The North Atlantic water settles in the circulating current zone southwest of Spitsbergen and enters the Arctic Ocean through the middle and deep layers, thus agreeing closely with the observed data (Hunkins 1990).
- Circulation in the Fram Strait is represented schematically in Fig. 19 described by Hunkins(1990), Paquette (1985), based on measurement. The model results resembles the situation of Fig. 19.
- East of Greenland, there exists a stream flow equivalent to the East Greenland Current.
- Density differences between the fresher Arctic Ocean and more saline Atlantic Ocean are considered to be the primary driving force.

(2) Bering Strait exchange (Figs. 13, 14 (1) and 18)

The northward flow through the shallow and narrow Bering Strait connects the Pacific (Bering Sea) and Arctic (Chukchi Sea)

oceans. Coachman and Aagaard (1981) note that the flow through Bering Strait is driven by a mean sea level slope of order 10^{-6} down toward the north, due to an effect related to the lower density of the Pacific relative to the Atlantic.

(3) Barents Sea and Kara Sea (Figs. 14(1) and 17)

- In the Barents Sea, the water mass which has come out of the Norwegian Sea joins the water mass coming out of the Kara Sea and the water coming out of the Pechora River while circulating counterclockwise in the central part of the Barents Sea, and flows westward to the south of Spitsbergen.
- This current agrees closely with the observed data, though there is some difference in position.
- In the western Kara Sea, the water mass which has come eastward from the polar point joins the water mass from the Kara Sea (fresh water mass from the Yenisey River and Ob River) and flows southward to the Barents Sea.
- If the flows obtained in the local field and regional field are

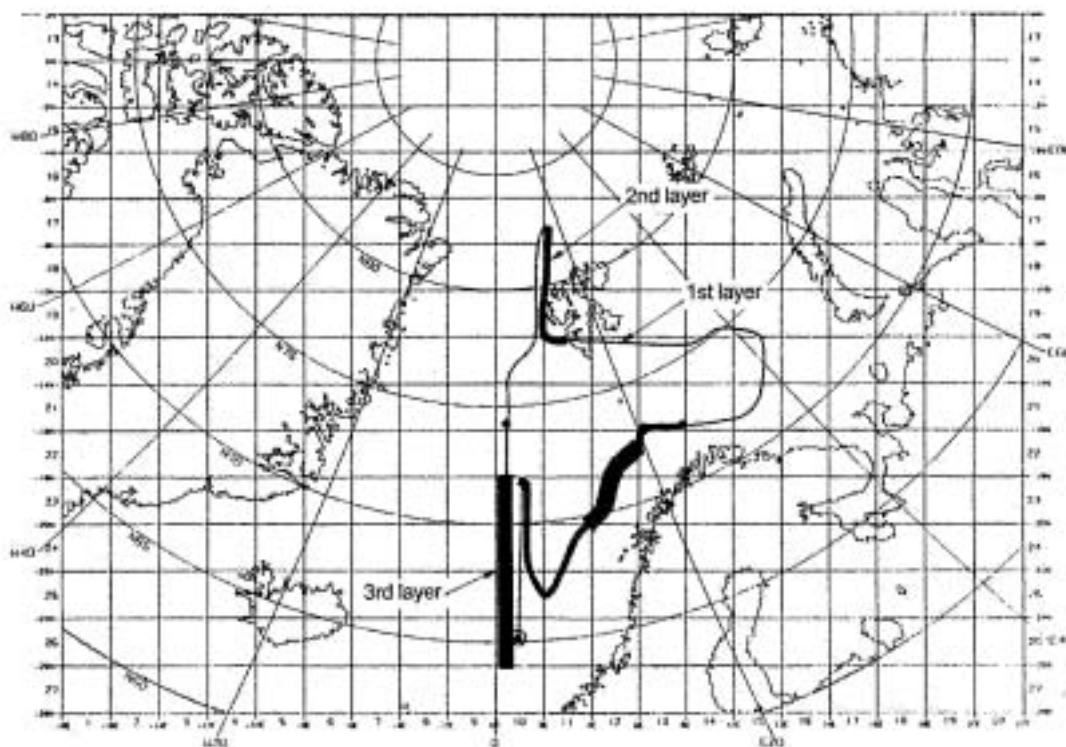


Fig. 17. Schematic diagram of vertical flows in the Arctic Ocean

compared, some difference is recognized in the flow patterns due to difference in grid size. Generally speaking, however, no difference is recognized in the results between models.

(4) Arctic Ocean

- In the surface layer of the Arctic Ocean, anticyclonic circulating current in the Canadian Basin is recognized as seen Fig. 14 (1) and 18.
- In the second and third layers, part of the water mass which has entered from the Norwegian Sea circulates cyclonically in the Arctic Ocean, the opposite direction to that of the Arctic water above it. It closely agrees with the circulation route (estimated) of the North Atlantic Ocean water in the intermediate and deep layers of the Arctic Ocean (Schlosser et al. 1995, Gerdes and Schauer 1997).

Due to the paucity of high-quality deep data, the sense of circulation in the deep layers is not well established. Aagaard, Carmack (1989) and Smethie et al. (1988) deduced from mooring and tracer data a cyclonic flow around the Eurasian basin.

- After circulating in the Arctic Ocean, water enters the Norwegian Sea again from the northeast coast of Greenland, which agrees with the observed data (Pickard and Emery 1990).

Consistency with the local model (Kara Sea, Barents Sea)

The author compared the results of flow analyses with the local model and the results obtained with the regional model. Both models agree that Atlantic Ocean water enters the Barents Sea along the Norwegian Peninsula, circulates counterclockwise in the Barents Sea and enters the Arctic Ocean and Norwegian

seas again. Both models reproduce the current which enters from the Arctic Ocean and the current which flows into the Barents Sea between Franz-Josef and Novaya Zemlya. The consistency between the two models is high.

Conclusions

The results of flow analysis may be summarized as follows:

- 1) Flows in the Barents Sea are affected by inflows from the neighboring seas (North Atlantic Ocean, Arctic Ocean). Inflow of river water from the Ob, Yenisey, etc. has the largest effect on changes in flows in the Kara Sea.
- 2) Flows obtained with the hybrid box model agree with flows based on observed data. For the deep layers, it will be necessary to carry out further studies on the reproducibility of flows because only a small amount of Arctic deep data are available.
- 3) The tracking of particles was performed with respect to calculated flows. This enabled to obtain a three-dimensional movement of particles with reproducibility of high accuracy.
- 4) The migration routes of cod were compared with the results of flow analysis. High similarity was recognized.
- 5) The Arctic Ocean presents a very dynamic circulating system. It encompasses the North Atlantic Ocean water which flows northward in the Norwegian Sea and river water coming out of major rivers.

A numerical hybrid box model was developed. The results reproduced many of the observed features such as the currents described below.

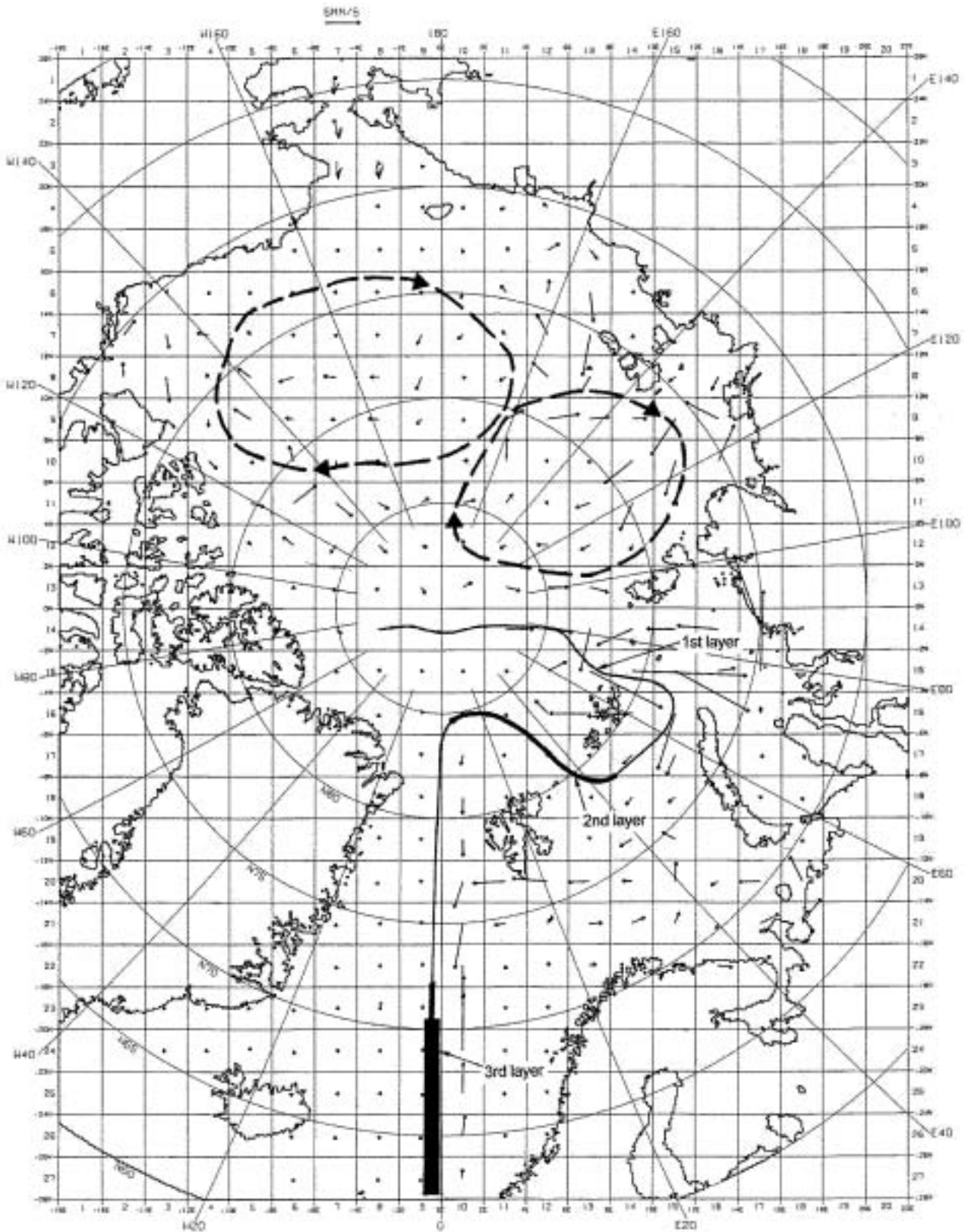


Fig. 18. Tracking of seawater particle and horizontal flow (surface layer).

Particularly, stream flows in the Norwegian Sea, Barents Sea and Kara Sea agree closely with the observed data. The flow field in the surface layer of the Arctic Ocean agrees with the observed data. In the intermediate and deep layers, the flow agrees with the observational data (counterclockwise circulation of North Atlantic water). Offshore, east of Greenland, flow equivalent to the Green-

land current is seen. The method of analysis used in this research was aimed at determining the flow field on the basis of observational data such as water temperature and salinity. Therefore, the importance of this data is unfathomable. Most notably regarding the Arctic Ocean, the availability of oceanographical data is very limited in compar-

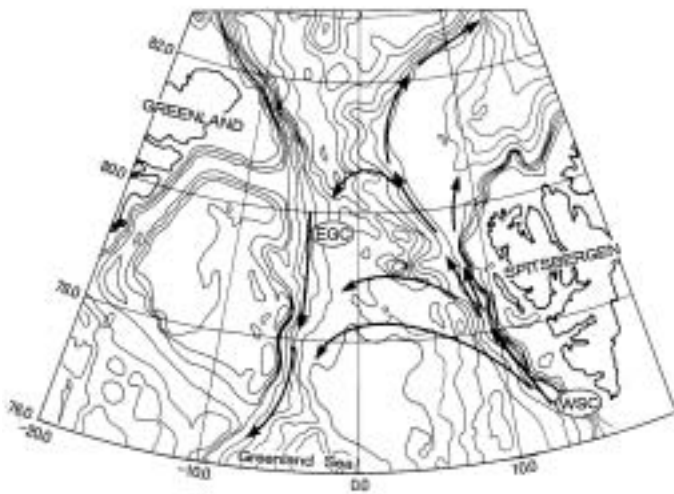


Fig. 19. Schematic circulation in Fram Strait (Gascard, J.C. et al. 1995).

ison with other seas, so that further accumulation of data is required.

Acknowledgements

This research work was supported by the Science and Technology Agency of Japan. The author is grateful to Mr. Teruo Hozumi of Ark Information System and Mr. Tairyu Takano of Suiken Kagaku Consultants Co., Ltd. for their assistance in the computational work and data processing. Thanks are also due to Dr. E. Zuur, Limnocéane, Université de Neuchâtel, who is one of the IAEA's multidisciplinary team of scientists, for his helpful advice in mathematical development in the course of carrying out this project.

Notations

- C : Specific heat of seawater
- E : evaporation
- H : heat
- P : precipitation
- p : pressure
- R : inflow of river water
- S : salinity
- T : water temperature
- W_{ij} : exchange flow rate from box i to box j
- ρ : density of seawater

References

[1] AAGAARD, K. and E. C. CARMACK (1989). The role of sea ice and other fresh water in the Arctic circulation. *Journal of Geophysical Research*, 94 (C10): 14485-14498.

[2] EMERY, W. J. and R. E. THOMSON (1998). *Data Analysis Methods in Physical Oceanography*. Pergamon.

[3] GERDES, R. and U. SCHAUER (1997). Large – scale circulation and water mass distribution in the Arctic Ocean from model results and observations. *Journal of Geophysical Research*, 102: 8467-8483.

[4] GASCARD, J. C., C. RICHEZ and C. ROUAULT (1995). New Insight on Large – Scale Oceanography in Fram Strait: The West Spitzbergen Current. *Coastal and Estuarine Studies*, Vol 49: 131-182, American Geophysical Union.

[5] GJEVIK, B. and T. STRAUME (1989). Model simulations of the M_2 and the K_1 tide in the Nordic Seas and the Arctic Ocean. *Tellus*. 41A: 73-96.

[6] HARMS, I. H. (1992). A numerical study of the barotropic circulation in the Barents and Kara Seas. *Continental Shelf Research*, 12.9: 1043-1058.

[7] HUNKINS, K. (1990). A review of the physical oceanography of Fram Strait. *The physical Oceanography of Sea Straits*: 61-93.

[8] International Atomic Energy Agency (1998). *Radiological Conditions of the Western Kara Sea, Report on the International Arctic Seas Assessment Project (IASAP)*

[9] LAWSON, C. L. and R. J. HANSEN (1995). *Solving Least Squares Problems*. SIAM (Society for Industrial and Applied Mathematics), Philadelphia, Prentice – Hall, INC.

[10] LOENG, H., E. SAKSHAUG, C. C. E. HOPKINS and N. ORITSLAND (1991). Features of the Physical Oceanographic Conditions of the Barents Sea. *Polar Research*. 10 (1): 5-18.

[11] MASLOV, N. A. (1944). The bottom-fishes of the Barents Sea and their fisheries, *Trudy PINRO, M.- L. Y. III.*: 3-186 (in Russian).

[12] PAQUETTE, R., R. BOURKE, J. NEWTON and W. PERDUE (1985). The East Greenland Polar Front in autumn. *Journal of Geophysical Research*, 90 (c3): 4866-4882

[13] PAVLOV, V. K. and S. L. PFIRMAN (1995). Hydrographic Structure and variability of the Kara Sea: Implications for pollutant distribution. *Deep – Sea Research*, 42.6: 1369-1390.

[14] PICKARD, G. L. and W. J. EMERY (1990). *Descriptive Physical Oceanography, An Introduction*. 5th Edition, Pergamon. 214-216.

[15] SCHLOSSER, P., J. H. SWIFT, D. LEWIS and S.L. PFIRMAN (1995). The role of the large-scale Arctic Ocean circulation in the transport of contaminants. *Deep – Sea Research*. 42 (6): 1341- 1367.

[16] SMETHIE, W. M. Jr, D. W. CHIPMAN, J.H. SWIFT and K. F. KOLTERMAN (1988). Chlorofluoromethanes in the Arctic Mediterranean seas, *Deep Sea Research*. 35: 347- 369.

[17] TAKAHASHI, Y. and A. WADA (1999). Study on Flow in the Sea of Japan by Box Model. *Journal of Hydroscience and Hydraulic Engineering, JSCE*. 17 (2): 139-158.

[18] WADA, A., Y. KINEHARA and T. TAKANO (1997). Marine contamination in the Arctic Ocean. *Journal of Global Environmental Engineering, JSCE*. 3: 37- 51.

[19] WADA, A., T. TAKANO and T. HOZUMI (1996). Estimation method for Residence Time of Bay Water. *Journal of Hydroscience and Hydraulic Engineering, JSCE*, 14 (1): 57- 66

[20] WALKER O. SMITH, Jr. (1990). *Polar Oceanography, Part A, Physical Science*, XV, Academic Press, Inc.

[21] WATABE, N., Y. KOHNO, D. TSUMUNE, T. SAEGUSA and H. OHNUMA (1996). *An Environmental Impact Assessment*

for Sea Transport of High Level Radioactive Waste. RAMTRAN, 7 (2/3): 117-127

[22] WUNSCH, C. (1996). The Ocean Circulation Inverse Problem. Cambridge University Press.

Appendix

Solving method for the hybrid box model

Solution of obtaining the exchange flow rates by means of a compartment model is identical with solving a quadratic programming problem so as to minimize the objective function under the condition of non-negativity of exchange flow rate, \underline{W} . That is,

Objective function (square of residual norm): $\|A\underline{W}-\underline{b}\|^2$, and
Constraint: $\underline{W}=0$,

where

- A: $m \times n$ matrix of coefficients, determined by observation data,
- \underline{b} : m -dimension constant vector determined by boundary conditions,
- \underline{W} : n -dimension vector of exchange flow rates,
- $\| \cdot \|$: Euclidean norm,
- m : number of conservation equations, and
- n : number of exchange flow rates.

Mathematically, this problem is called convex quadratic programming problem or NNLS (Non Negative Least Squares).

Background of solution

In general, the number of exchange flow rates, n , is less than that of equations, m , and solutions of such a problem are easily obtained either by general inverse matrix or by nonlinear programming method without constraints. However, some of exchange

flow rate values thus obtained could be negative, which makes difficult to interpret the solutions as physical phenomena.

To overcome this difficulty, an effective program was developed based on a solution algorithm in which the problem was formulated as convex quadratic programming problem with a constraint of nonnegative exchange flow rates.

Solution processes

Algorithm of the active set method is premised on three points as follows:

- (1) When all of exchange flow rates are 0, it satisfies the equations and constraint,
- (2) Solution of quadratic programming problem without constraint can be obtained by the usual least squares method, and
- (3) Criteria of optimum solution are given by the Kuhn-Tucker's condition that is usually applied in quadratic programming method.

Outline of the algorithm for obtaining optimum solution is summarized as follows:

- First, let all elements of exchange flow rate be 0, and select an element W_q that leads to the optimum solution most closely;
- Solve the quadratic programming problem without constraint, and correct the resulting solution so as to fulfill the non-negativity restraint;
- Using the corrected solution, solve again quadratic programming problem without constraint, and correct solution that does not satisfy the non-negativity constraint; and
- When the non-negativity constraint is fulfilled, select another element of exchange flow rate that has been set to be 0, and repeat the procedures above, thus decreasing one by one the number of elements set to be 0, until the optimum solution is reached.